1

Concepts of Gas–Liquid Flows

1.1. Introduction and basic concepts

Two-phase convection is a specific domain of convective transfers. It is mainly of interest for two industrial fields, the chemical industry and especially the petrochemical industry, where distillation is the basic process. It is also of interest for the nuclear industry, which for several decades has catalyzed the research in this field. Nuclear research centers (such as CENG in France) and global electricity producers (EDF) are leaders in this field. For this industry, transfer efficiency is the objective.

The interest of the two-phase transfer will be briefly explained. Increasing the temperature of one kilogram of water by $\Delta T = 100\ C$ requires an amount of heat $\Delta Q_1 = 4180*100 = 4.18.10^6\ J$. Evaporating the same mass requires $\Delta Q_2 = m\ L = 2.09.10^6\ J$, which adds to the heat transfer when the heated water is evaporated.

This theoretical and practical interest is compensated by an increased complexity of the phenomena and their prediction.

The authors feel that it advisable to provide a overview, if not a culture, on this specific field, which is important in terms of the technical and economic stakes of the subject. Even less so than in other contexts, this overview does not pretend to be exhaustive, or to serve as training for specialists.

For a color version of all the figures in this chapter, see: www.iste.co.uk/ledoux/heat4.zip.

Any reader interested in further information should dive into the rich but complex literature. The reference section to this book includes a deliberately limited number of references, which provide a solid basis and a convenient starting point for conducting research that may prove to be full of surprises.

Since the reader may lack the skills required for the calculation of a nuclear power plant, this part of the book focuses on the presentation of the basic concepts.

A distinction must be made between liquid and vapor flows, in which gas is generated in the liquid phase, and sprays, in which the liquid phase is generated externally and carried by a gas flow.

1.2. Gas–liquid flows

The following presentation focuses on forced convection in a vertical tube. The research and design of installations involve the consideration of various questions:

a) From the point of view of physics and thermodynamics

– The experiments for the characterization of two-phase flows generally proceed by the simultaneous introduction of a piping by two flow rates of liquid and gas determined by the experimenter.

– In the heat transfer, vapor results from heat input. The “quality” is determined by the transfer phenomenon, of which it is an integral part.

The fairly complex “boiling” processes must then be taken into account first. Other interacting phenomena are those related to the gas–liquid equilibrium and capillarity. They are dealt with in the section introducing the concept of nucleate, saturated or unsaturated flow.

b) From the point of view of fluid mechanics

– The coexistence of two phases, liquid and vapor (often vapor of liquid), requires a reconsideration of the flow structure. Various structures notably appear as a function of the flow “quality” (this term will be explained in what follows). An a priori distinction must be made between ascending vertical flows, descending vertical flows and horizontal flows. It is also worth mentioning, without going into detail, the case of annular flows, which occur in certain heat exchangers.

– Every flow of real fluid involves a loss of energy by friction, which is referred to as head loss in fluid mechanics. Here again, the calculation of head loss of a two-phase flow through the pipe (as well as in annular space) is needed.

c) From the point of view of heat transfer between a fluid and the wall of a piping system

– A general theme of the problem is presented by relying on the "pool boiling" phenomenon; see section 1.2.1.4.

– Then the calculation of diffusive convective heat transfer is approached. The presentation is deliberately focused on the seemingly most common case of a vertical tube with constant heat load.

Beyond acquiring "basic knowledge" on the subject, the reader is expected to be motivated to follow a literature research on an exciting but complex subject.

1.2.1. *The physics of two-phase flows*

1.2.1.1. *Review of thermodynamics: liquid–vapor equilibrium*

The following is a review of a thermodynamics lecture dedicated to the liquid–vapor equilibrium. The reader may complete it by revisiting previous courses.

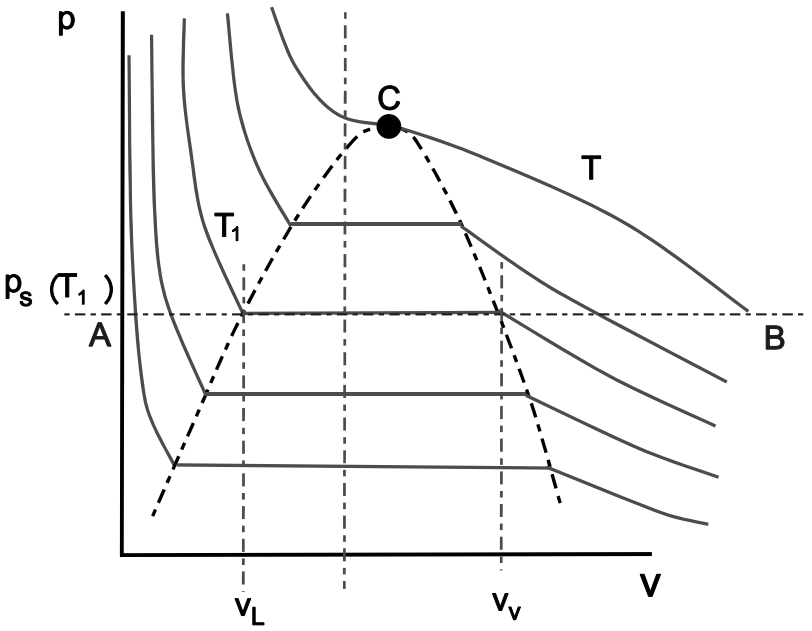

Figure 1.1. *Clapeyron diagram: Andrews' isothermals*

Let us consider a *Clapeyron diagram*, which for a pure substance represents the relation between its specific volume and its pressure.

The specific volume v, or the volume per unit mass, therefore expressed in $m^3\ kg^{-1}$ is the inverse of density ρ: $v = \frac{1}{\rho}$.

The **Clapeyron diagram** is composed of isothermals, which are commonly known as the *Andrews' isothermals*. It can be noted that each isothermal passing below point C reaches a plateau. All the plateaus belong to a dotted curve. The left part of this curve is known as the *boiling point curve*, while the right part is the *dew point curve.*

Each isothermal cutting the dew point curve has three parts:

– a left part, where the body is in the liquid state: this is referred to as compressed liquid;

– a right part where the body is in the gaseous state: this is referred to as vapor;

– a plateau limited by the boiling/dew point curve: on this plateau, the liquid and gaseous phases coexist; their dosage determines the specific volume. At the left end of the plateau $v = v_L$, where v_L is the specific volume of the liquid under pressure p_S and temperature T. At the right end of the plateau $v = v_V$, where v_V is the specific volume of the liquid under pressure p_S and temperature T.

The pressure of a plateau is known as the saturation vapor pressure p_S. It is a direct function of the temperature of the isothermal characterizing the plateau: $p_S = p_S(T)$.

It is possible to move along a horizontal line AB (which is therefore isobaric), for example, by modifying the volume of fluid, which is accompanied by a heat transfer, or to determine the phase change by a heat transfer, which involves a change of specific volume. From A to B, there is a succession of compressed liquid, an area of equilibrium between mixture and vapor increasingly richer in gas to the right, and then gas.

The passage of a mass m from the liquid state to the vapor state on the saturation plateau requires an amount of heat L. Expressed in C, L is the heat of

vaporization (or specific enthalpy of vaporization Δh_V, as this heat is provided under constant pressure, which is the saturation vapor pressure p_S).

Clapeyron established a significant relation between the heat of vaporization, the specific volumes of the two phases and the differential of the saturation vapor pressure with respect to temperature:

$$\frac{dp_{Sat}}{dT} = \frac{L}{T\left(v_V - v_L\right)} \qquad [1.1]$$

This formula can be used to calculate the heat of vaporization based on the data provided by the Clapeyron diagram.

At a point C, the isothermal is tangent to the dew point curve. In this case, the plateau is reduced to a point. C is known as the ***critical point***. The isothermals below this point correspond to a state of dense matter, a fluid that is neither liquid, nor vapor, its state being referred to as the ***supercritical state***.

This critical point is characterized by a critical pressure p_C and a critical temperature T_C, which are highly variable from one fluid to another.

Several examples are listed below:

Water: $p_C = 22.12\ MPa$ and $T_C = 374.15\ C$

Methane: $p_C = 4.6\ MPa$ and $T_C = -82.6\ C$

Carbon dioxide: $p_C = 7.29\ MPa$ and $T_C = 31.3\ C$

1.2.1.2. *Capillarity*

The presence of gases and liquids coexisting in a flow leads to the presence of interfaces. The existence and deformation of these interfaces give rise to forces, known as interface forces or capillary forces. Although weak, these forces play a first-order role in the dynamics of bubbles and pockets whose existence will be subsequently described.

Capillary forces occur as soon as an interface is stretched. These forces have their origin in molecular interactions and they compensate in volume. Each molecule is “pulled in every direction by its neighbors”. At an interface, the symmetry is broken and intermolecular forces become manifest.

The fundamental law can be written as the expression of the force F needed to stretch a length l of the interface:

$$F = \sigma l \qquad [1.2]$$

here, σ is the surface tension.

It is a quite weak coefficient expressed in $N.m^{-1}$. Its value for water at $T = 20\ C$ is generally considered $\sigma = 7.210^{-2}\ N.m^{-1}$. This value should be considered with caution. In fact, at temperature

$T = 0\ C$, its value is $\sigma = 7.56410^{-2}\ N.m^{-1}$

and at $T = 37\ C$, it is $\sigma = 710^{-2}\ N.m^{-1}$

The accuracy of these figures may be misleading. They are valid for very clean water. The slightest impurity, unavoidable in many practical cases, leads to a decline of the value, which may reach $\sigma = 6.510^{-2}\ N.m^{-1}$ or even less in the case of notable pollution.

It is important to note that force is not proportional to the stretch, as it is for a spring. The force remains the same irrespective of stretch, until breakage. On the other hand, the force is proportional to the length of the stretched interface.

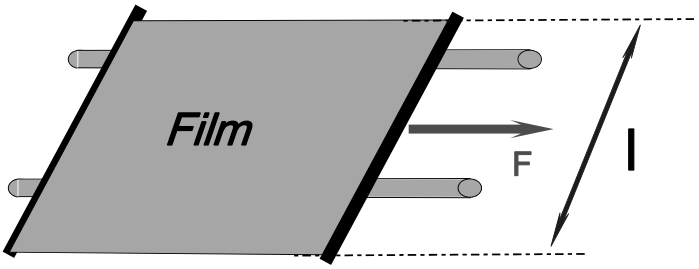

Figure 1.2. *Capillarity: stretching of a liquid film*

This is often illustrated by showing the stretching of a plane film over a length l . The force is then:

$$F = 2\sigma l \qquad [1.3]$$

the coefficient 2 in this formula results from the existence of ***two*** interfaces.

In the physics of two-phase systems, interfaces of interest have a spherical geometry. In this case, a pressure difference occurs when crossing the interface. The internal pressure at the concave face is higher than the external pressure, irrespective of the fluids.

According to Laplace, in general terms, when crossing an interface, there is a pressure variation that can be written as follows:

$$\Delta p = p_i - p_e = \sigma \left(\frac{1}{R_1} + \frac{1}{R_2} \right) \qquad [1.4]$$

p_i is always the internal pressure in the concavity and $\frac{1}{R_1} + \frac{1}{R_2}$ is an invariant of a point of the surface. R_1 and R_2 are the radii of curvature on two planes perpendicular to one another.

For a spherical interface of radius R, the Laplace formula is written as:

$$\Delta p = p_i - p_e = \frac{2\sigma}{R} \qquad [1.5]$$

Three common cases can thus be considered:

– A gas bubble of radius R surrounded by liquid:

$$\Delta p = p_i - p_e = \frac{2\sigma}{R}, \qquad [1.6]$$

as there is a single interface to be crossed;

– A “free” bubble, composed of a spherical liquid thin film enclosing gas. The two gas–liquid and liquid–gas interfaces can then be assumed to have the same radius R

$$\Delta p = p_i - p_e = \frac{4\sigma}{R} \qquad [1.7]$$

as there are two interfaces to cross;

– A drop, liquid sphere of radius R

$$\Delta p = p_i - p_e = \frac{2\sigma}{R} \qquad [1.8]$$

as there is a single interface to cross.

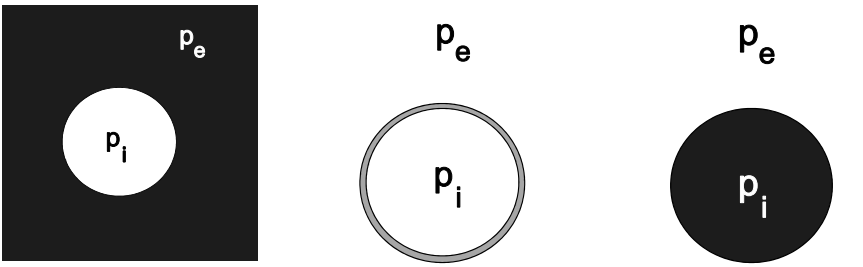

Bubble: one interface $\Delta p = p_i - p_e = \frac{2\sigma}{R}$

Bubble: two interfaces $\Delta p = p_i - p_e = \frac{4\sigma}{R}$

Drop: one interface $\Delta p = p_i - p_e = \frac{2\sigma}{R}$

Figure 1.3. *Capillarity. Drops and bubbles: various interface topologies*

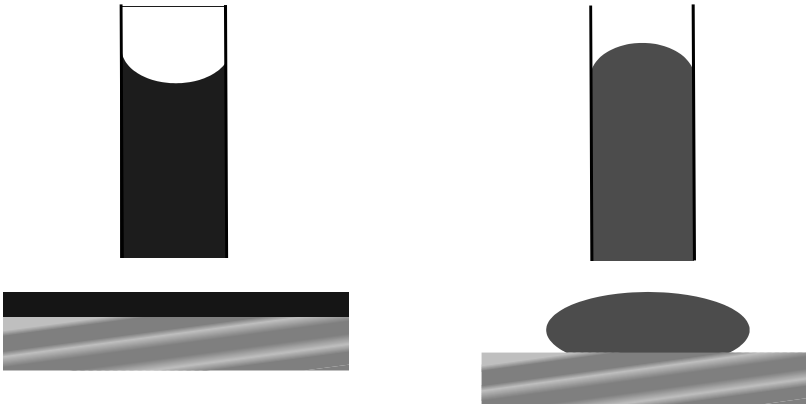

Water: concave meniscus, film

Mercury: convex meniscus, deformed drop

Figure 1.4. *Film and drop menisci*

The behavior of fluid molecules in the presence of a solid depends on the considered liquid. For example, water tends to extend over a solid. On a flat surface,

this gives rise to a film, and in a tube, to a concave meniscus. On the other hand, a molten metal, such as mercury, tends to "flee" from the solid. For a drop, this leads to a contact angle, depending on the weight of the drop and the forces of attraction of the fluid surface under the drop (but the calculation of this angle may prove to be burdensome), and, in a pipe, there is a concave meniscus.

Finally, if a small diameter tube is plunged into a tank filled with water, a rise of the liquid in the tube can be noted. The height h of water above the free surface of the liquid is given by ***Jurin's law.*** When the forces (capillarity, weight of the column, pressure force on fluid interfaces) are in equilibrium, the height h is written as:

$$h = \frac{4\sigma}{\rho g D} \qquad [1.9]$$

where D is the inner diameter of the tube and σ is the surface tension constant for water–air.

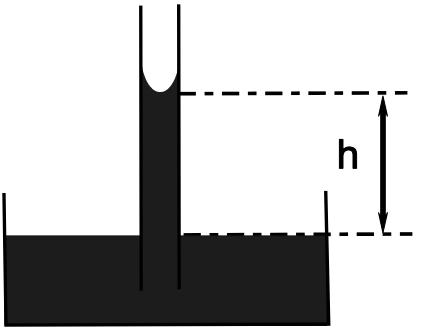

Figure 1.5. *Jurin's law* $h = \frac{4\sigma}{\rho g D}$

1.2.1.3. *Bubble dynamics*

Bubble flows are widely present among liquid gas flows. The formation of bubbles and the evolution of their size represent a wide range of significant problems in the processes.

Moreover, flows may travel through piping systems featuring cross-sectional changes or pipe accidents giving rise to significant pressure variations.

The technological impact of these problems is the object of an active fundamental research field. This quite subtle physics is generally little known, and largely ignored by the literature.

The in-depth study of this domain is beyond the scope of this book. Mentioning it here, together with its most outstanding results, appeared to be a necessity. This may motivate any interested reader to refer to the literature, most often under the title of Cavitation (see, in particular, the collective work by J.P. Franc et al. entitled *Cavitation. Physical Mechanisms and Industrial Aspects* [FRA 95]).

Two types of phenomena motivate these studies:

– the occurrence of vapor by heating of the liquid, or boiling;

– the occurrence of vapor by reduction of the pressure in the liquid, or cavitation.

The transition from liquid into vapor at the core of a liquid is more complex in practice. It involves the production, and growth of bubbles, which is the boiling phenomenon.

Bubble formation requires the temperature to reach, for a given pressure of the liquid, the saturation temperature corresponding to this temperature $T_{Sat}(p)$. In fact, the required temperature gap $\Delta T = T - T_{Sat}$ should be at least $\Delta T = 5\,C$.

The creation of a bubble in a liquid involves the existence of a seed. The seed is often a micro-volume of gas adsorbed in the crevices of the surface of the heating element (micro-cracks, etc.). The micro-bubble is thus able to grow.

Indeed, theoretically speaking, the diameter of a bubble should be zero at its creation, which would mean infinite internal pressure or, at least, for a bubble of very small diameter, an extremely high pressure. A bubble would therefore occur as a consequence of the inclusion of gas that is foreign to the vapor and partly insoluble.

Two problems arise:

– Bubble size evolution depending on external pressure stresses. This is expressed here by the Rayleigh–Plesset equation.

– Evolution of a bubble inside which the liquid vapor and a foreign gas coexist. This is expressed here by Blake's theory.

a) The dynamics of a bubble subjected to an ambient pressure (external to the bubble) that varies in time is a complex problem, in the realm of unsteady fluid mechanics, which must simultaneously take into account viscosity forces and surface tension forces. The equation describing this is known as the **Rayleigh–Plesset equation**, and sometimes as the **Besant–Rayleigh–Plesset equation.**

This equation has the form of the Navier–Stokes equation in spherical coordinates, in the hypothesis of spherical symmetry.

It is a relatively complex second-order nonlinear differential equation:

$$R\frac{d^2R}{dt^2}+\frac{3}{2}\left(\frac{dR}{dt}\right)^2+\frac{4\nu_L}{R}\frac{dR}{dt}+\frac{2\sigma}{\rho_L R}+\frac{\Delta p(t)}{\rho_L}=0 \qquad [1.10]$$

where:

$R(t)$ is the sought-for time evolution of the radius of the bubble.

ρ_L and ν_L are respectively the density and the kinematic viscosity of the liquid in which the bubble is immersed. σ is the surface tension between the liquid and the vapor surrounding the bubble.

$\Delta p(t) = p_\infty - p_i$ is the pressure differential between the internal pressure in the bubble p_i, assumed to be known and $p_\infty(t)$ the pressure "far" from the bubble, which is imposed.

The resolution in $R(t)$ gives the evolution of a bubble subjected to a variation of ambient pressure.

This resolution is complex. Simplifying hypotheses are sometimes used, notably assuming that the liquid is a perfect fluid ($\nu_L = 0$).

It is important to note that when Δp is fixed, the radius Δp no longer varies with time. The context is then that of fluid statics, and the Laplace formula is:

$$\frac{2\sigma}{\rho_L R}+\frac{\Delta p}{\rho_L}=0 \qquad [1.11]$$

or:

$$p_i - p_\infty = \frac{2\sigma}{R} \qquad [1.12]$$

b) Blake's theory (1949)

Blake was interested in the static equilibrium of a cavitation bubble. This is how he was able to explain the unstable character of this phenomenon.

Consider the existence in the liquid of a very small bubble, known as a seed, a sphere of radius r and filled with gas and vapor. Blake's innovative idea was to assume that this very small vapor bubble is polluted by a gaseous impurity.

Consider a seed containing liquid vapor at pressure p_V and a foreign gas at pressure P_G.

At equilibrium, the following can be written as:

$$p_i - p_\infty = \frac{2\sigma}{R} \qquad [1.13]$$

where:

$$p_i = p_G + p_V \qquad [1.14]$$

or:

$$p_\infty = p_G + p_V - \frac{2\sigma}{\rho_L R} \qquad [1.15]$$

where pressure p_V is a saturation vapor pressure. Assuming that temperature is constant, it is fixed.

On the other hand, p_G varies with volume and therefore with the radius R of the bubble.

Consider R_0, the radius of the bubble at the beginning of a process, and p_{G0}, the pressure of the gas for this radius. For another radius R, the following can be written as:

$$\frac{p_G}{p_{G0}} = \left(\frac{R_0}{R}\right)^3 \qquad [1.16]$$

which is the expression of Boyle–Mariotte's law under constant temperature.

The relation between pressure p_∞ and radius $R(p_\infty)$ is therefore given by:

$$p_\infty = p_{G0}\left(\frac{R_0}{R}\right)^3 + p_V - \frac{2\sigma}{R} \qquad [1.17]$$

When R increases, this curve is asymptotic to $p_\infty = p_V$:

– this can be deduced from:

$$p_\infty = p_{G0}\left(\frac{R_0}{R}\right)^3 + p_V - \frac{2\sigma}{\rho_L R} \text{ when } R \text{ tends to infinity;} \qquad [1.18]$$

– the curve of variation of p_∞ with R depends on the rate of foreign gas present in the bubble. For a given value of p_{G0}, this curve descends to a minimum, referred to as critical.

A critical value of radius R_C is thus obtained:

$$R_C = \sqrt{\frac{3\,p_{G0}\,R_0^3}{2\sigma}} \qquad [1.19]$$

and a critical value of the pressure:

$$p_C = p_{G0}\left(\frac{R_0}{R_C}\right)^3 + p_V - \frac{2\sigma}{\rho_L R_C} = p_{G0}\frac{2\sigma R_0^3}{3\,p_{G0}R_0^3} + p_V - \frac{2\sigma}{R_C}. \qquad [1.20]$$

or:

$$p_C = p_V - \frac{4\sigma}{3R_C} \qquad [1.21]$$

Below this pressure, and above this value of the radius, the radius of the bubble cannot be given by the static solution. Depending on the experimental conditions, a bubble explosion is generally possible.

1.2.1.4. *Nucleate boiling*

In Andrews' experiments, when pressure conditions at constant temperature change, a liquid–vapor equilibrium can be reached without difficulty in practice. This equilibrium results from an evaporation or condensation at an interface in a piston–cylinder system.

The evaporation or condensation at an interface is one of the ways in which the passage between liquid and vapor states occurs in practical systems. This occurs at the free surface of films.

This bubble generation is known as nucleate boiling. It is an essential mechanism in the two-phase heat transfer through pipes. As already noted, a minimum requirement for boiling is the saturation temperature. In a pipe subjected to a heat flux, a thermal gradient is established in the fluid, temperature decreasing starting from the wall. When a thermal regime sets in, the core of the fluid may remain at a temperature below a temperature gap $\Delta T = T - T_{Sat}$ while this temperature may exceed a temperature gap $\Delta T = T - T_{Sat}$ in the area near this wall. Nucleate bubbles may then form at the wall. This is referred to as *subcooled nucleate boiling.* If all the liquid has a temperature equal to or higher than a temperature gap $\Delta T = T - T_{Sat}$, this is referred to as *saturated nucleate boiling.*

Our objective is to present here an empirical approach to the heat transfer in a vertical tube. However, for a better understanding of the problems involved by this transfer, the results of the study of heat transfer during *pool boiling* are presented.

Consider a setup in which a volume of liquid is in a container. This liquid is heated, either through a wall, or in practice by an electrical heating element (immersion heater). The process is similar in practice to that occurring in a pressure cooker or a domestic electric water heater. It is important to note that interesting phenomena occur at the surface of the heating source.

Based on this already quite old experiment conducted by Nukiyama [NUK 66], the differential of the wall temperature of the heating element T_W and of the saturation temperature $\Delta T = T_W - T_{Sat}$ is represented in the abscissa. On the ordinate, there are the heat flux density T_W transmitted to the fluid and the convection coefficient $h = \dfrac{\varphi_W}{T_W - T_O}$, where T_O is the fluid core temperature.

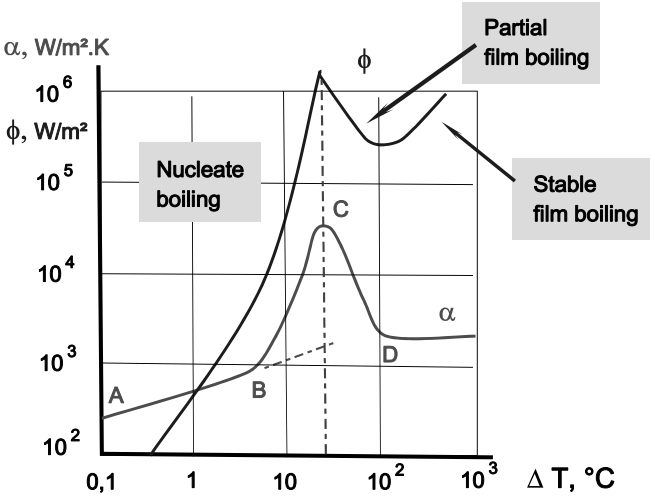

Figure 1.6. *Heat transfer in pool boiling*

The curve of the convection coefficient can serve as a guide. It is important to note the presence of several zones, therefore heating regimes, varying with the temperature differential controlled by the wall temperature:

From **A** to **B**, there is natural convection in a single phase liquid.

From **B** to **C**, there is nucleate boiling. As noted above, this point is situated at a differential $\Delta T = 5\,C$.

In **C**, there is a transfer peak. At this point, steam generation is such that it destabilizes the liquid film: the solid interface is partly covered by a vapor film. The convection coefficient and consequently the flux are limited by this vapor film whose thermal resistance is higher than a liquid convection coefficient.

An unstable liquid film can be noted from **C** to **D**, leading to a fluctuating contact between the wall and the gas and the liquid. As the proportion of vapor increases, the flux decreases with temperature.

Finally in **D**, a continuous vapor film is formed, the convection coefficient is stabilized and the flux can then increase again with the temperature differential.

1.2.2. *Classification of flows*

Many studies were conducted without heating in "two-phase loops" where the liquid and gas flow rates are controlled. Flow quality is thus imposed as an experimental parameter. This research method can be used to reproduce flow types that are naturally generated along a vertical or horizontal tube, when it is heated. In a heated vertical tube, there can be a succession of various characteristic types of flow, whose rate is higher as the heating gets stronger.

Ascending vertical flows

– Bubbly flow. Bubbles can be independent or gathered in clusters.

– Plug flow or slug flow, where the gas plugs are carried by the flow. It can be noted that these plugs are rounded at the top and rather flat at the bottom.

– Annular flow. The liquid forms a film along the wall. A continuous central flow of air extracts drops from this film. Several transition phases can be noted, a quite chaotic *churn* flow, then a film flow and a *dispersed flow*, in which the drops sometimes gather in "clusters" and is referred to as *wispy flow*.

Horizontal flows

When the gas flow rate increases, the following types of flows can be successively noted in a horizontal tube:

– A bubbly flow. The gas is contained in the liquid flow body in the form of bubbles.

– A slug flow or plug flow in which bubbles have coalesced and given rise to slugs.

– A stratified flow, where the flows of gas and liquid are continuous and superimposed. At this stage, the interface is calm.

– A wavy flow. The speed difference between gas and liquid deforms the interface and gives rise to waves.

– A slug flow. The amplitude of waves is sufficient to reach the upper part of the tube and slugs are once again formed.

– An annular flow. An annular liquid film is crossed by a continuous flow of gas. The drops extracted from the film by instability form a cloud at the center of the gas flow.

A descending vertical flow features aspects that have already been mentioned with the ascending tube, with several variants:

– bubbly flow;

– slugs;

– falling film: when the flow rates are low, the liquid descends along the wall in a film. Obviously, this configuration cannot be observed in ascending flow, where the only way the film can be generated is by the effect of the viscosity of the gas flow;

– bubbly falling film;

– churn flow;

– dispersed annular flow.

Typology of two-phase flows

In two-phase flow, the geometry of the interfaces between vapor and liquid comes under different forms (surfaces of films, bubbles, slugs). This leads us to determine various typologies, also referred to as two-phase flow topologies. Only pipe flows are covered here. Given the large difference in density between vapor and liquid (typically from 10 to 10^3 depending on the pressure in a section), gravity has a strong influence and requires a distinction being made between ascending and descending vertical flows, as well as horizontal flows. Annular tubes and spaces should also be distinguished.

Although all geometries may be present in real heat exchangers, this book focuses on ascending tubes. However, for the reader's information, indications will be given on descending and horizontal flows.

The motivation for the numerous experiments conducted in order to identify these flows is given by the necessity to identify, classify, and predict the occurrence of flowing typologies. They are also an experimental support for the modeling and prediction of the mechanics of fluids and two-phase transfers.

As already mentioned, for any reader with a desire to specialize in this domain, this chapter can only be an introduction to a more complete literature.

Parameters

The parameters determining a flow that are most commonly indicated in the publications are the following:

Mass flow rate of the liquid: q_{mL}

Mass flow rate of the vapor: q_{mV}

(Actual) mass quality

$$x = \frac{q_{mV}}{q_{mV} + q_{mL}} \quad [1.22]$$

Volume flow rate of the liquid: q_{VL}

Volume flow rate of the vapor: q_{VV}

Volume quality

$$\beta = \frac{q_{VV}}{q_{VV} + q_{VL}} \quad [1.23]$$

Surface rates

$$J_V = \frac{q_{mV}}{\rho_V S} \quad [1.24]$$

$$J_L = \frac{q_{mL}}{\rho_L S} \quad [1.25]$$

“Mass rates” are also considered:

$$\dot{m}_V = \frac{q_{mV}}{S} = \rho_V J_V \quad [1.26]$$

$$\dot{m}_L = \frac{q_{mV}}{S} = \rho_L J_L \qquad [1.27]$$

The following expression can be written as:

$$q_m = q_{mV} + q_{mL} \qquad [1.28]$$

hence:

$$x = \frac{q_{mV}}{q_m} \qquad [1.29]$$

and:

$$q_{mV} = x\, q_m \qquad [1.30]$$

which leads to:

$$J_V = x_V \frac{q_m}{\rho_V} \qquad [1.31]$$

Ascending vertical flow

Various topologies are represented in Figure 1.7.

The best known flow is the *bubbly flow*. When their density increases, upon cold increase of the initial gas flow rate, or they appear during heating in the presence of heat transfer, these bubbles interact strongly and a *packed bubbly flow* can be noted.

Due to their interaction under high density conditions, bubbles coalesce and a *slug flow* can be noted. At this level, there is a distinction between plug flow and slug flow. Plug designates here a volume, a gas pocket. It appears that putting several plugs end to end results in a long pocket whose oscillating behavior recalls the advancement of a slug.

Increasing the vapor rate flow leads to a film flow; this takes place through a chaotic destabilization leading to a *churn flow* configuration. An annular flow is thus obtained.

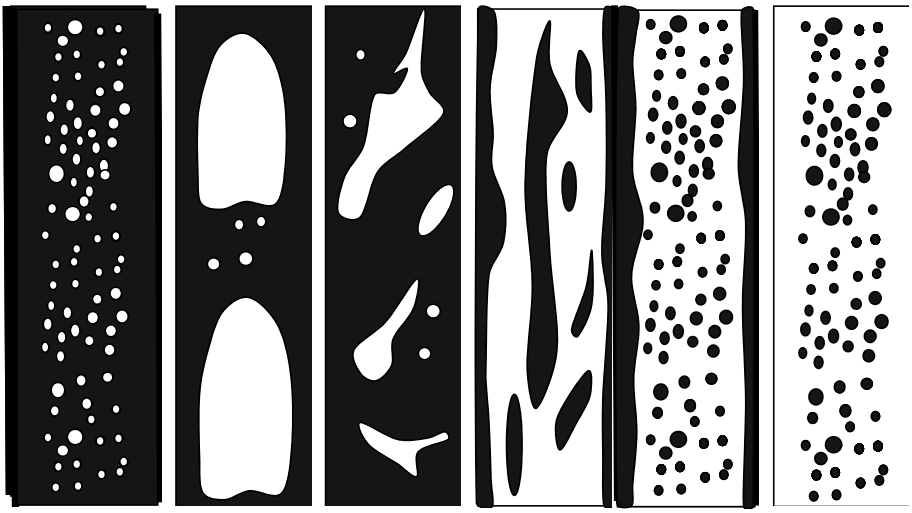

1) Bubbly flow

2) Slug flow

3) Churn flow (shaked)

4) Churn flow (chaotic)

5) Bubbly film

6) Dispersed annular flow

Figure 1.7. *Ascending vertical flow*

Descending vertical flows

These flows are represented in Figure 1.8.

Bubbly flows and slug flows occur, and a film flow emerges. This is a falling film this time.

This falling film evolves into a bubbly film. Due to churn, it may evolve into a dispersed annular flow. In this case, the velocity differential between vapor and liquid allows a surface sputtering and the gas flow carries a mist.

It is important to note a particular phenomenon, which occurs when an ascending vapor flow emerges. If the velocity of this flow is sufficient, the gas–liquid interfacial friction is significant and tends to bring up the film. This phenomenon, which may be annoying in the installations, is referred to as "*flooding*".

1) Bubbly flow

2) Slug flow

3) Falling film

4) Bubbly film

5) Churn flow

6) Dispersed annular flow

Figure 1.8. *Descending vertical flow*

Horizontal flow

Various topologies are presented in Figure 1.9.

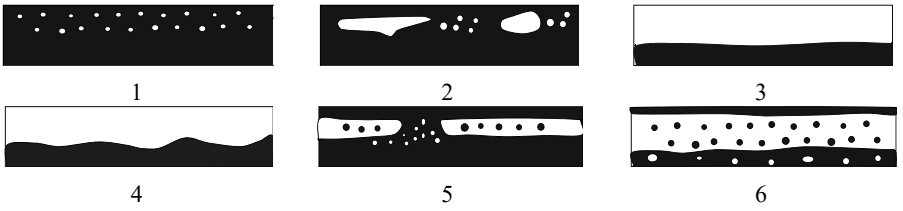

1) Bubbly flow

2) Plug flow

3) Stratified flow

4) Wavy flow

5) Slug flow

6) Annular flow

Figure 1.9. *Horizontal flow*

Due to gravity, there is a certain stratification of flows.

First, there are *bubbly flows* and a *plug flow* carrying slugs. As can be noted, the gaseous phases tend to concentrate on the upper part of the tube.

From the same perspective, a stratified flow can be noted.

For quite high values of gas velocities, the interface becomes undulated. This is the *wavy flow.*

Since the amplitude of waves increases with gas velocity, the crest of the waves reaches the upper wall of the tube, and a *slug flow* emerges.

This flow may evolve into an annular flow, where the extraction of drops leads to a mist carried by the gaseous phase.

Validity areas of these flows

Identification works, relying on visualizations, are doubled given the necessity to predict the occurrence of these various typologies. The literature on this subject is quite rich, so only references will be provided here. Focusing on the vertical pipe flows, one of the methods for predicting the occurrence is presented here. Similar to the others, it relies on a diagram for positioning the experimental operating point of a flow on a diagram. The parameters on these scales vary from one author to another.

The Hewitt and Roberts method [HEW 69] is presented here. It relies on experiments conducted on the air/water couple up to 59 bar, and water vapor/liquid water up to 69 bar.

The various flow structures (patterns) are located in the areas of a diagram having:

– for the abscissa:

$$\rho_L J_L^2 = \frac{\overline{G}^2 (1-\beta)^2}{\rho_L} \qquad [1.32]$$

– for ordinate:

$$\rho_G J_G^2 = \frac{\overline{G} \beta^2}{\rho_G} \qquad [1.33]$$

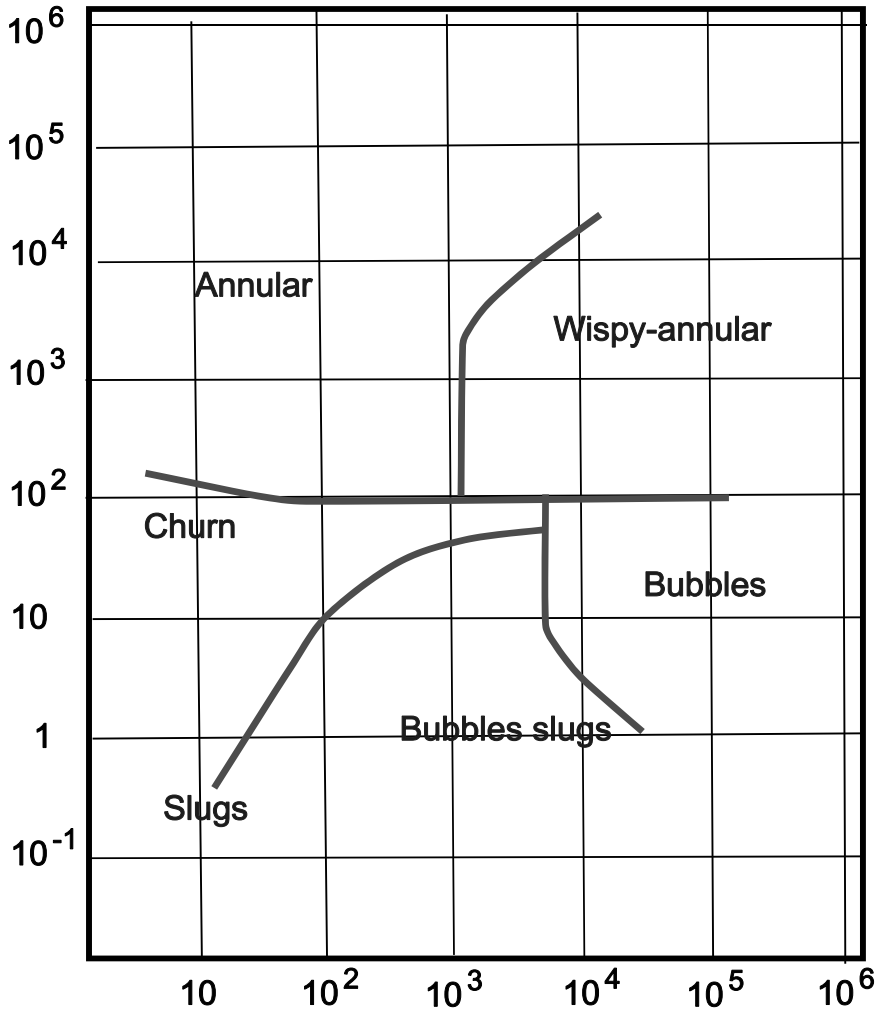

Figure 1.10. *Diagram* in the abscissa: $\rho_L J_L{}^2 = \dfrac{\bar{G}^2(1-\beta)^2}{\rho_L}$;

in the ordinate $\rho_G J_G{}^2 = \dfrac{\bar{G}\beta^2}{\rho_G}$

1.2.3. *Topologies of a heated vertical flow*

Various types of flow that may occur in a vertical tube have been described. As already mentioned, in fundamental studies, the flow is most often obtained by controlling the quality (ratio of mass flow rates of gas and liquid). The gas is most often air, distinct from the liquid vapor.

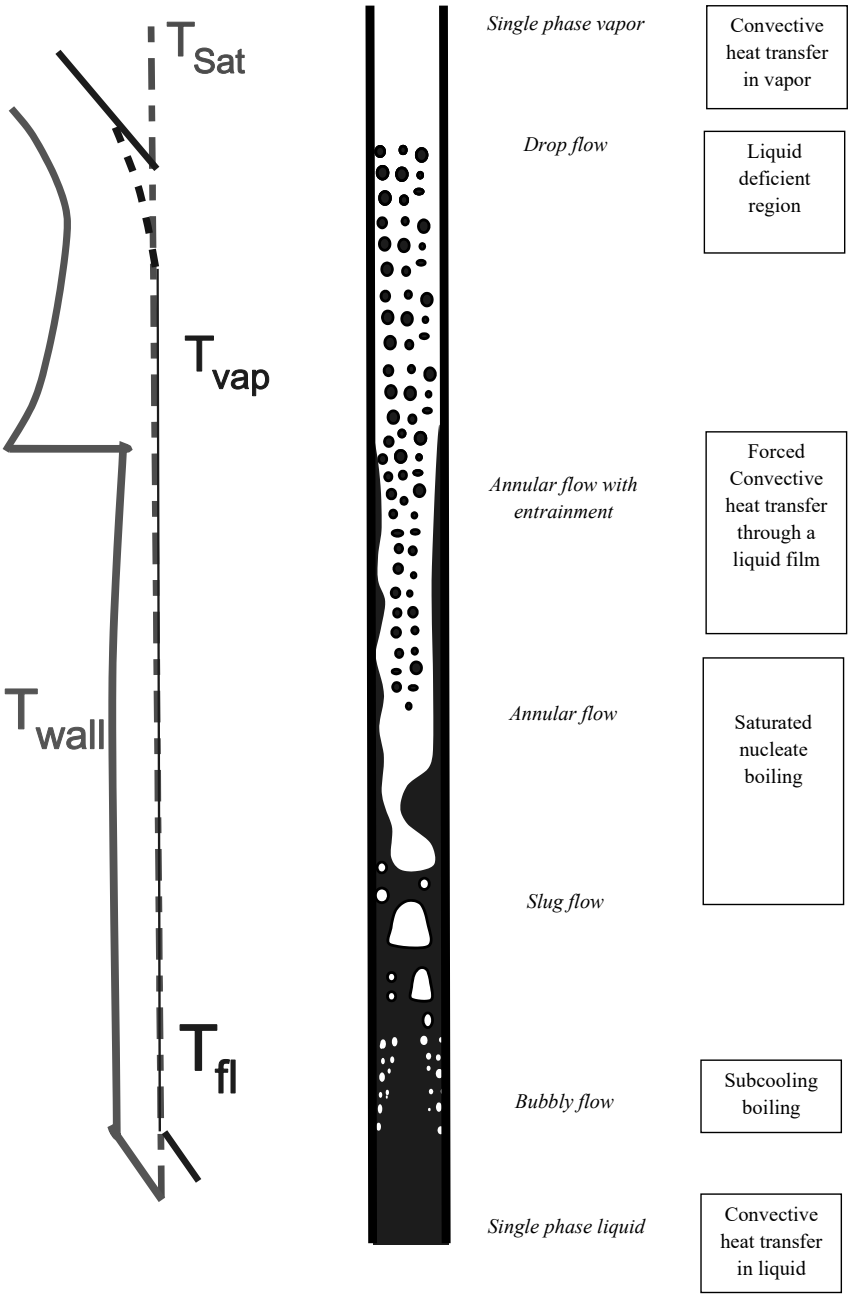

Figure 1.11. *Ascending vertical flow. Flow topologies and transfer zones*

In the case of a heated tube through which there is an initially liquid, therefore single phase, flow, the various phases of the flow and the various structures (flow patterns) of this flow are determined by the evolution, the history of the heating. Flow structures follow one another from the bottom to the top of the tube, all of them being interdependent, in the "history" of the heated flow.

Not all the structures are present, their occurrence depending on the length of the tube and the imposed heat load.

They are presented using a schematic representation that is quite commonly present in one form or another in various treatises.

The case considered here is that of a wall transfer at constant flux density φ_W .

The occurring flow structures (patterns) are successively analyzed, followed by the types of heat transfer involved, and finally a schematic representation of the forms taken by the distribution of wall and core temperature is provided.

From the bottom to the top of the tube

A single phase zone (liquid flow) remains at a temperature below the saturation temperature T_{Sat} (temperature of the liquid–vapor equilibrium plateau of Andrews' isothermals). It is important to note that the effect of heating is a parallel increase of the wall and core temperatures. As long as no point of the liquid reaches the temperature T_{Sat} , the flow remains single phase.

A nucleate boiling zone:

– given the thermal gradient controlling the transfer, the temperature T_{Sat} will be reached close to the wall before the axis and the bubbles will form at the wall. In this first zone, the density of the bubble remains moderate and localized near the wall, with a migration;

– when the temperature reaches (and exceeds) T_{Sat} throughout a section, there is bubbly flow throughout the tube.

Slug flow: as the density of bubbles increases, their interactions are strong, and they then coalesce into slugs.

Annular flow: as they grow, these slugs also coalesce and they generate a liquid film flow surrounding an inner gas flow. For mass conservation reasons, the inner velocity of the gas exceeds that of the film (slowed down, among others, by the viscosity at the wall) and this film is referred to as entrained. The velocity difference

between vapor and liquid also leads to a destabilization of the interface (Kelvin–Helmholtz instability) and the formation of a cloud of drops carried by the gaseous flow.

Drop flow: at the interface of the film, there is skimming by atomization and also evaporation. The liquid rate flow of this film will therefore decrease, the film thickness will decrease from bottom to top, until they disappear. There only remains a drop flow that evaporates until it becomes a single-phase flow, this time a vapor flow.

The disappearance of the film is, both literally and figuratively, a catastrophe. Indeed, it leads to a sudden discontinuity of the convection coefficient T_{Sat}, which decreases drastically. The flux being conserved, the temperature differential strongly increases (the schematic representation is resented further). This differential is reflected by the wall temperature, whose integrity may be compromised.

This phenomenon is known as *dry out*. The consequences in various industrial installations, particularly in the nuclear field, can only be imagined.

This is designated by terms such as boiling crisis, critical heat flux (CHF), departure from nucleate boiling (DNB) or burnout (BO).

From a thermal point of view, various transfer zones can be qualified based on these flow structures:

– zone of convective heat transfer between the wall and the liquid;

– zone of subcooled boiling corresponding to wall boiling;

– zone of saturated nucleate boiling, joining the developed bubbly flow and the slug flow zone;

– zone of forced convective heat transfer through the liquid film;

– zone of flow in the absence of liquid, joining evaporating drop flow and pure vapor.

Temperature profiles

A general form of temperature profiles can be logically deduced.

Recalling that flux density is constant: the zone of liquid convection leads to a parallel increasing evolution of the wall and fluid temperatures.

Since the occurrence of saturated nucleate boiling, the fluid temperature remains constant and equal to T_{Sat}. In the annular and film zones, the decrease of the film

leads to a decrease of the thermal resistance. The wall temperature slightly decreases.

At dry out, the drastic decrease of the convection coefficient leads to an increase of thermal resistance and, the vapor remaining close to T_{Sat}, to a sudden and significant increase in the wall temperature.

Finally, the return to a two-phase flow leads to a parallel evolution of the wall and core temperatures.

Definition of quality

Given the mass flow rates of the vapor and the liquid, denoted by q_{mV} and q_{mL} respectively, in a tube section, the quality x is defined by:

$$x = \frac{q_{mV}}{q_{mV} + q_{mL}} \qquad [1.34]$$

It can also be shown that:

$$x = \frac{h(z) - h_L}{L} \qquad [1.35]$$

where L, h_V and h_L are respectively the heat (enthalpy) of vaporization and the specific enthalpies of vapor and liquid; $h(z)$ is the specific enthalpy in the considered section, of altitude z.

1.2.4. *Calculation of fluxes*

Each flow structure leads to a different formulation for the calculation of wall flux. The literature on this subject is quite complex. A selection is proposed here.

Single-phase flow

$$\Delta T = T_W - T_L(z) \qquad [1.36]$$

$$\varphi_W(z) = h_{L0}\left[T_W - T_L(z)\right] \qquad [1.37]$$

Dittus and Boelter

$$Nu_D(z) = \frac{h_{L0}(z)D}{\lambda_L} = 0.023\, R_D^{0.8}\ \mathrm{Pr}_L^{\frac{1}{3}} \qquad [1.38]$$

where R_D is the Reynolds number of the liquid flow:

$$R_D = \frac{V_{qL}\,D}{\nu_L} = \frac{\dot{m}_L\,D}{\mu_L} = \frac{q_{mL}\,D}{S\,\mu_L} \qquad [1.39]$$

where S is the cross-section of the tube and $\dot{m}_L$ is the "mass rate" of the liquid

$$\dot{m}_L = \rho_L V_{qL} = \frac{q_{mL}}{S} \qquad [1.40]$$

and the Prandtl number of the liquid:

$$\mathrm{Pr}_L = \frac{\nu_L}{a_L} = \frac{\mu_L\, c_{pL}}{\lambda_L} \qquad [1.41]$$

The Dittus–Boelter formula does not take into account the viscosity variation due to the temperature on a section.

The Sieder–Tate formula may be preferred, which calculates the Nusselt number by:

$$Nu_D = \frac{h_L\,D}{\lambda_L} = 0.023\ \mathrm{Pr}^{\frac{1}{3}}\, R_D^{0.8} \left(\frac{\mu}{\mu_W}\right)^{0.14} \qquad [1.42]$$

which leads to

$$h_L = 0.023 \frac{\lambda_L}{D}\, \mathrm{Pr}^{\frac{1}{3}}\, R_D^{0.8} \left(\frac{\mu}{\mu_W}\right)^{0.14} \qquad [1.43]$$

The two formulas differ only by the term $\left(\frac{\mu}{\mu_W}\right)^{0.14}$

The use of this term leads to an iterative process in the calculation of the variation of the axial temperature. It is important to note, for example, that at $p = 15\ bar$ for respective temperatures at the wall and the core $T_W = 200\ C$ and $T_L = 100\ C$, the ratio is $\frac{\mu}{\mu_W} = \frac{1.39.10^{-4}}{2.82.10^{-4}}$ and the term $\left(\frac{\mu}{\mu_W}\right)^{0.14}$ is equal to 0.905 which is a 10% gap between the two formulas.

Subcooled nucleate boiling

ONB = Onset of boiling

Bergles and Rosenhow [BER 64]

$$\left(T_W - T_{Sat}\right)_{ONB} = 0.556 \left(\frac{\varphi_W}{1082\, p^{1.156}}\right)^{0.463\, p^{0.0334}} \qquad [1.44]$$

David and Anderson [DAV 66]

$$\left(T_W - T_{Sat}\right)_{ONB} = \left(\frac{8\sigma\varphi_W\, T_{Sat}}{\lambda L \rho_V}\right)^{0.5} \qquad [1.45]$$

To extend this to liquids other than water, Frost and Dzacovic propose the multiplication of this formula by the Prandtl number of the liquid:

$$\left(T_W - T_{Sat}\right)_{ONB} = \left(\frac{8\sigma\varphi_W\, T_{Sat}}{\lambda L \rho_V}\right)^{0.5} \mathrm{Pr}_L \qquad [1.46]$$

The transfer is then calculated with the same convection coefficient as for pure liquid, but the temperature difference is recalculated in an adapted manner:

$$\varphi_W(z) = h_{L0}\left[T_W - T_L(z)\right] = h_{L0}\left[\left(T_W - T_{Sat}\right)_{ONB} + \left(T_{SAT} - T_L(z)\right)\right] \qquad [1.47]$$

Fully developed subcooled boiling

The wall flux density (heat load) is imposed.

The wall temperature is expressed as a function of the wall flux density and pressure:

$$T_W(z) = T_W(\varphi_W, p) \qquad [1.48]$$

Rosenhow [ROS 52]:

$$\frac{c_p\ \Delta T_{Sat}}{L} = C_{FSB}\left[\frac{\varphi_W}{\mu_L\ L}\left(\frac{\sigma}{(\rho_L - \rho_V)g}\right)^{0.5}\right]^{0.33} \mathrm{Pr}_L^{1.7} \qquad [1.49]$$

C_{FSB} is a constant that varies according to the authors, depending on the experimental data used to establish a correlation.

The presence of the surface tension can be noted, which highlights the influence of nucleation in the physical process. Similarly, the constant varies depending on the nature of the metallic material of the wall.

Without pretending to be exhaustive, an example is provided below for a heat transfer with water:

Geometry	**Nature of the tube**	C_{FSB}
Vertical tube $D = 4.56\ mm$	Stainless steel	0.06
Vertical tube $D = 27.1\ mm$	Copper	0.013
Horizontal tube $D = 14.9\ mm$	Stainless steel	0.015
Horizontal tube $D = 2.39\ mm$	Stainless steel	0.020

Jen and Lottes [JEN 51] for water:

$$\Delta T_{Sat} = 25\ \rho_W^{0.25} \exp\frac{-p}{62} \qquad [1.50]$$

(p in atmospheres), modified by Thom:

$$\Delta T_{Sat} = 22.65\ \rho_W^{0.5} \exp\frac{-p}{87} \qquad [1.51]$$

valid for the ranges $115 - 340\ C$, $7 - 172\ bar$ and $11 < \dot{m} < 1.05.10^4\ kg.m^{-2}.s^{-2}$.

Saturated nucleate boiling

Consider simply

$$T_L(z) = T_{Sat} \qquad [1.52]$$

The wall temperature becomes independent of $\dot{m}$ and x .

The limit between *saturated nucleate boiling* and the *two-phase forced convective region* is determined by a critical value of the wall flux density

$$\varphi_{W,ONB} = \frac{8 h_{TP}^2\ \sigma T_{Sat}}{\lambda_L\ L\ \rho_V} \qquad [1.53]$$

Here, h_{TP} is the convection coefficient in the two-phase forced convective region.

Two-phase forced convection region

The flow takes the form of an annular film

$$\frac{h_{TP}}{h_{L0}} = f\ \frac{1}{X_{tt}} \qquad [1.54]$$

Here, X_{tt} is the Martinelli coefficient for turbulent flows of liquid and gas (double index tt).

Related to the head losses $X_{tt} = \dfrac{\Delta p_L}{\Delta p_V}$

X_{tt} can be calculated by:

$$X_{tt} = \left(\frac{1-x}{x}\right)^{0.9} \left(\frac{\rho_V}{\rho_L}\right)^{0.5} \left(\frac{\mu_L}{\mu_V}\right)^{0.1} \qquad [1.55]$$

Forms of the function:

Dengler [DEN 56]:

$$\frac{h_{TP}}{h_{L0}} = 3.5\left(\frac{1}{X_{tt}}\right)^{0.5} \quad [1.56]$$

Guerrieri and Talty [GUE 56]:

$$\frac{h_{TP}}{h_{L0}} = 3.4\left(\frac{1}{X_{tt}}\right)^{0.45} \quad [1.57]$$

Bennett [BEN 61]:

$$\frac{h_{TP}}{h_{L0}} = 0.564\left(\frac{1}{X_{tt}}\right)^{0.74} \varphi_W^{0.11} \quad [1.58]$$

Schrock and Grossman [SCH 62]:

$$\frac{h_{TP}}{h_{L0}} = \gamma\left[\frac{\varphi_W}{\dot{m}\,L} + m\left(\frac{1}{X_{tt}}\right)^n\right] \quad [1.59]$$

with

$\gamma = 7.39.10^3$

$m = 1.5.10^{-4}$

$n = 0.66$

values of Wright, suggested by Collier:

$\gamma = 6.70.10^3$

$m = 3.5.10^{-4}$

$n = 0.66$

Other approaches

The following formulas are valid for the zones of saturated nucleate boiling and the two-phase forced convection region.

Chen:

$$h_{TP} = h_{NCB} + h_C$$

where h_{NCB} is the convection coefficient calculated for nucleate boiling and h_C is given by:

$$h_C = 0.023 \left[\frac{\dot{m}(1-x)D}{\mu_L} \right]^{0.8} \mathrm{Pr}_L^{0.4} \frac{\lambda_L}{D} F(X_{tt}) \qquad [1.60]$$

This recalls the formulas for single-phase convective heat transfer, with a modified Reynolds number and a corrective function $F(X_{tt})$.

$F(X_{tt})$ is given in the form of a curve that can be replaced by the expression:

– for $X_{tt} < 0.1$: $F(X_{tt}) = 1$ [1.61]

– for $X_{tt} > 0.1$: $F(X_{tt}) = 2.35 \left(\frac{1}{X_{tt}} + 0.213 \right)^{0.736}$ [1.62]

Forster and Zuber proposed the calculation of h_{NCB} by:

$$h_{NCB} = 1.22.10^{-3} \frac{\lambda_L^{0.79} c_{pL}^{0.45} \rho_L^{0.49}}{\sigma^{0.5} \mu_L^{0.29} L \rho_V^{0.24}} \Delta T_{Sat}^{0.24} \Delta p_{Sat}^{0.75} S \qquad [1.63]$$

where S is given by a curve that can be expressed by:

$$S = \left(1 + 2.53.10^{-6} R_{eL}^{1.17}\right)^{-1} \qquad [1.64]$$

Post dry out

Groeneveld

$$Nu_V = a\left[\mathrm{R}_{eV}\left[x+\frac{\rho_V}{\rho_L}(1-x)\right]\right]^{-b}\ \mathrm{Pr}_{V,W}^{c}\ Y^{d} \qquad [1.65]$$

with

$$Y = 1-0{,}1\left(\frac{\rho_L}{\rho_V}-1\right)^{0.4}(1-x)^{0.4} \qquad [1.66]$$

then:

$a = 1.09.10^{-3}$

$b = 0.985$

$c = 1.41$

$d = -1.15$

Slaghterback [SLA 71]:

$$Nu_V = a\left[\mathrm{R}_{eV}\left[x+\frac{\rho_V}{\rho_L}(1-x)\right]\right]^{-b}\ \mathrm{Pr}_{V,W}^{c}\ \ \varphi_W^{d}\ \left(\frac{\lambda_V}{\lambda_{V,BO}}\right)^{e} \qquad [1.67]$$

It is important to note an uncommon expression, where the Nusselt number depends on the flux density, which is also part of its definition.

Here, $\lambda_{V,BO}$ is the heat conductibility at “burn out” and

$a = 1.16.10^{-3}$,

$b = 0.838$,

$c = 1.81$,

$d = 0.278$,

$e = 0.508$.

1.3. Dispersed phase flows: mists and sprays

In the broad sense, two-phase flows can be divided into two categories: pipe flows, bubbly flows, slug flows or a more complex combination of film and drop flows with dispersed phase: mists and sprays

1.3.1. *Mist*

A mist is a suspension in a gaseous fluid, possibly in a moderate flow of a cloud of drops or droplets of moderate density.

If the liquid phase and possibly the gaseous phase have a strong impulse, then it is a spray. The second category is of interest here.

Sprays have a particular place in the field of fluid mechanics and heat engineering.

In the absence of heat incidence, they relate to fluid mechanics, and are the subject of various chapters:

– the theory of instabilities for their formation;

– the particular transport by a flow, which is most often turbulent;

– possibly the theory of jets, if the cloud impulse is sufficient to drive a significant flux of air.

The presence of thermal phenomena can take various forms, a non-exhaustive list of which is as follows:

– Spray vaporization; a drop may evaporate in a calm gaseous atmosphere, or in a gaseous flow with relative velocity. The convective heat transfer between the gas and the drop is then considered in the calculation.

– Combustion of drops, distinguishing between the combustion of the individual drop and the combustion of an oxidized mixture resulting from the prevaporization of spray.

– Interaction of the spray with a solid surface: spray cooling phenomena, for example, metal quenching.

Finally, it is important to note that in certain topologies of tube flow, there are zones of mist, their formation requiring a destabilization of the liquid–gas interface of a film.

Sprays are quite common in daily life and in the industrial field. In the absence of heat engineering, there are cosmetic and pharmaceutical applications. In the industrial world, spray is important in combustion phenomena, being present in the field of industrial combustion, internal combustion in cars, aircraft and spaceship engines.

Sputtering is in fact a must for burning liquids. Combustion is a phenomenon occurring exclusively in gaseous phase. Any liquid needs to be vaporized to undergo the chemical process of combustion. The burnt quantity is proportional to a volume, and the evaporated quantity is proportional to a surface. The division into droplets optimizes this vaporization by increasing the ratio of the evaporation surface S to the volume V to be burnt; for a drop of diameter d :

$$S = \pi \frac{d^2}{4} \qquad [1.68]$$

$$V = \pi \frac{d^3}{6} \qquad [1.69]$$

$$\frac{S}{V} = \frac{\pi d^2}{4} \frac{6}{\pi d^3} = \frac{3}{2d} \qquad [1.70]$$

It can be seen that the ratio $\frac{S}{V}$ is in $\frac{1}{d}$; it is therefore optimized for the small droplets. Moreover, it can be shown that a combustion time of the drops is proportional to d^2.

This explains why the purpose in combustion is to find the smallest possible size of the drops.

This subject cannot be extensively covered within the limited space of this book, but it seemed necessary to give the reader a minimal amount of information on a subject that has little attention paid to it in classical manuals.

The following section provides several notions on:

– the formation of sprays, the processes involved and the sputtering techniques;

– the characterization of a spray, or particle sizing;

– spray vaporization.

1.3.2. *Spray generation*

Spray generation involves a significant number of various devices, whose structure often depends on the industrial field concerned. A non-exhaustive list includes:

– car, aircraft and spaceship engine manufacturers;

– agriculture, for spreading insecticides;

– surface coverage technologies: paintings, surface treatments, etc.

The needs of these various domains differ. In order to optimize combustion, engine manufacturers are interested in decreasing vaporization times. Sprays of the smallest possible size are sought. Agriculture is most often interested in larger drops, which are less carried by the wind and offer a better coverage of foliage. Painting technology proposes the sputtering of products whose rheology may sometimes prove challenging.

Generally speaking, the production of sprays results from a flow instability.

The natural instability of a liquid cylinder, or the Rayleigh instability, is the prototype. Properly analyzed, it is rather a laboratory object, as the available flow rates are very small. It is, however, important to note that it is the only sputtering mode that generates single size drops.

The design of an atomizer is most often empirical. Generally speaking, an injector generates a sheet flow, a jet flow or another type of flow that tends to get destabilized. The flow may be naturally unstable (e.g. the conical sheet created by a household spray), or the instability may be promoted by the friction with a gaseous ambience or a gaseous flow.

A broad classification includes the mechanical injectors, which use the pressure of the liquid in a device whose geometry is apt to create an unstable flow, and aided injectors, in which the liquid flow is accompanied by a gaseous flow that tends to destabilize it.

1.3.3. *Spray characterization: particle sizing*

The drops that constitute a spray are never of the same size. Rayleigh instability is practically the only means to generate a one-dimensional spray. It is a laboratory device, quite delicate to implement in its controlled form, and which provides a very low flow rate.

In practice, the various sputtering processes produce polydisperse sprays.

They must be characterized by a statistical distribution of the size of drops.

Two types of information may be sought:

– the statistical law in detail;

– focus on mean diameters.

1.3.3.1. *Size distributions*

a) There are statistical distributions or probability function.

There are two main distributions: numerical and volumetric distributions.

The number fraction $f_n(x)$ is defined based on the number dn of drops whose diameter ranges between x and $x+\delta x$:

$$dn = f_n(x)\,\delta x \qquad [1.71]$$

The volume fraction $f_V(V)$ is defined based on the number dn_V of drops whose volume ranges between v and $v+\delta v$:

$$dn_V = f_V(v)\,\delta v \qquad [1.72]$$

By definition:

$$\int_0^\infty f_n(x)\,\delta x = 1 \qquad [1.73]$$

$$\int_0^\infty f_V(v)\,\delta v = 1 \qquad [1.74]$$

Cumulative laws are also defined.

For example, the volume cumulative $F_V(x)$ gives the fraction of liquid volume contained in the drops whose diameter exceeds the value x.

b) Mean diameters

Mean diameters can be defined using these distributions.

A mean diameter d_{pq} can thus be defined using the numerical distribution $f_n(x)$

$$d_{pq} = \int_0^{\infty} \left[\frac{x^p f_n(x)}{x^q f_n(x)} \right]^{\frac{1}{p\_q}} d x \qquad [1.75]$$

The main mean diameters used are:

– the numerical mean diameter d_{10}

$$d_{10} = \int_0^{\infty} x f_n(x) \delta x \qquad [1.76]$$

– the volume mean diameter d_{30}

$$d_{30} = \left[\int_0^{\infty} x^3 f_n(x) \delta x \right]^{\frac{1}{3}} \qquad [1.77]$$

– the Sauter mean diameter d_{32}

$$d_{32} = \int_0^{\infty} \frac{x^3 f_n(x)}{x^2 f_n(x)} \delta x \qquad [1.78]$$

This diameter is very common in the literature, especially in the fields of combustion and engines. It implicitly contains a coupling between the surface and the volume. It will be seen further on that evaporation is a surface phenomenon, while combustion depends on the fuel richness throughout volumes.

c) Various statistical laws were used, the most common of which are:

– ***Rosin–Rammler law***

Initially used to characterize coal aggregates, it is probably the most well-known and at any rate the oldest law.

It relies on volume cumulative

$$F_V\left(d < x\right) = \exp -\left(\frac{x}{\overline{X}}\right)^N \qquad [1.79]$$

This law features two parameters $\overline{X}$ and N. These two parameters, one having the dimension of a diameter and the other one being dimensionless, are sufficient to provide all the information on the relative distribution of drop sizes. This law is all the narrower as N is larger.

A numerical density can be deduced from it:

$$f_n = \frac{N x^{n-4}}{\left(\overline{X}\right)^{N-3} \Gamma\left(1-\frac{3}{N}\right)} \exp\left(\frac{x}{\overline{X}}\right)^N \qquad [1.80]$$

with Gamma function:

$$\Gamma\left(x\right) = \int_0^\infty t^{x-1}\, e^{-t} dt \qquad [1.81]$$

– ***Log-normal law***

This law, proposed by Mugele and Avans, uses an auxiliary variable:

$$Y = Ln\, x - Ln\, \overline{X} = Ln \frac{x}{\overline{X}} \qquad [1.82]$$

It is a numerical law:

$$f_n\left(x\right) = \frac{N}{\sqrt{\pi}} \exp - N^2 Y^2 \qquad [1.83]$$

Here, N is also an enlargement parameter.

Mean diameters are readily calculated:

$$d_{pq} = X \exp \frac{p+q-6}{4N^2} \qquad [1.84]$$

– ***Nukiyama–Tanasawa law***

This is a numerical density:

$$f_n = A\, x^2 \exp - \left(\frac{x}{\overline{X}} \right)^N \qquad [1.85]$$

For $N = 6$, it is similar to the Rosin–Rammler law.

Mean diameters can be calculated:

$$d_{pq} = \left(\overline{X} \right)^{p-q} \frac{\Gamma\left(\frac{p+3}{N} \right)}{\Gamma\left(\frac{q+3}{N} \right)} \qquad [1.86]$$

One variant is the ***Tanasawa–Tesima*** law:

$$f_n = A\, x^{\alpha} \exp - \left(\frac{x}{\overline{X}} \right)^{\beta} \qquad [1.87]$$

This law is similar to the **Weibull law**, which is common in the theory of reliability:

$$f_n = \left(\frac{x}{N} \right)^N \exp - \left(\frac{x}{\overline{X}} \right)^N \qquad [1.88]$$

d) Particle sizing has historically employed various metrology methods:

– The impaction method, derived from solid dust technologies.

– The photographic method: with large magnification with brief lighting (spark, then laser).

– Optical diffraction methods: the spray is dealt with similar to a pupillary function in a Fraunhofer setup. The difficulty is twofold: having an annular detector, which has been available for several decades now, and having a technique for the inversion of the diffraction figure, which was more challenging throughout history.

1.3.4. *Spray vaporization: the case of the isolated drop*

Mist vaporization is common in chemical engineering sciences and is systematically encountered in car or spaceship engines. Indeed, combustion is a phenomenon of gaseous phase and the introduction of a liquid fuel in a combustion chamber requires its preliminary vaporization. Calculating spray vaporization is therefore a must.

This type of calculation relies on the theory of vaporization of the isolated drop.

The Godsave model is a basis for this evaluation. It deals with vaporization controlled by the contribution of heat conduction or convection to the drop.

This model is not always sufficient. The problem is in fact complex. Vapor diffusion in the ambient atmosphere may oppose resistance to the transfer. Moreover, fuels that are commonly used in the automobile or aerospace fields are petroleum cuts, therefore mixtures of species. Other fuels are used in the aerospace industry: cryogenic fuels, sometimes in supercritical state, or propellants (containing the same oxidizing and fuel products).

To remain within the scope of this book, the focus here is on providing the results of Godsave's calculation.

This theory gives a law that is known as the D^2 -law.

The vaporization of the drop involves the decreases of its diameter in time. The model yields the following relation:

$$D^2(t) = D_0^2(t) - K\,t \qquad [1.89]$$

Constant K is calculated as follows:

$$K = 8\frac{\lambda_G}{c_{PG}\rho_L} Ln(1+B) \qquad [1.90]$$

where B, known as the Spalding parameter, is given by:

$$B = \frac{C_{PG}\left(T_V - T_a\right)}{L_V} \qquad [1.91]$$

The constant can be corrected in the presence of forced convection. Given Reynolds' values of drops in practice, laminar convection is assumed. The correction yields:

$$K_{conv} = K\ \left(1 + 0.3\, R_D^{0.5}\, \mathrm{Pr}^{1/3}\right) \qquad [1.92]$$

Whittaker proposed a more complex correction law, relying on a Nusselt number:

$$Nu_D = 2 + \left[\, 0.4\, R_D^{0.5} + 0.06\, R_D^{2/3} \,\right] P_r^{0.4} \left(\frac{\mu_e}{\mu_w}\right) \qquad [1.93]$$

$Nu_D = 2$ then corresponds to pure conduction without convection.

This formula would be valid for $3.5 < R_e < 80\,000$ and $0.7 < P_r < 380$.

The correction would then be:

$$K_{conv} = K\ \left(1 + \left[\, 0.2\, R_D^{0.5} + 0.03\, R_D^{2/3} \,\right] P_r^{0.4} \left(\frac{\mu_e}{\mu_w}\right)\right) \qquad [1.94]$$

1.4. Several examples

As already mentioned, the reader may lack the skills required to design a nuclear power plant or a refinery. In the absence of such skills, the reader would need to refer to a literature covering a wider range of knowledge. This includes in particular the calculation of complex two-phase transfers related to a specific numerical modeling (see [BER 81]).

Consequently, the following examples focus on the physics of two-phase systems and on sprays, domains that are somewhat ignored by certain textbooks.

EXAMPLE 1.1.– Determination of heat of vaporization

Using the tables provided by Appendix 3 and Clapeyron's formula, find the heat of vaporization of water under an atmospheric pressure of $1.013\,bar$ and at a temperature of $225\,C$. Compare it to the values given by the same tables.

SOLUTION TO EXAMPLE 1.1.–

The two chosen operating points correspond to two vaporization plateaus:

$$1\,bar = 10^5\ Pa = 0.1\,MPa$$

The plateau corresponding to $1\,bar$ is therefore characterized by

$$p = 1.013\,MPa$$

$$T = 100\,C$$

The plateau corresponding to $225\,C$ is characterized by

$$p = 2.548\,MPa$$

$$T = 225\,C$$

Recalling Clapeyron's formula:

$$\frac{d\,p_{Sat}}{d\,T} = \frac{L}{T\left(v_V - v_L\right)} \qquad [1.95]$$

Working on a table, the pressure derivative must be calculated using the "finite differences" method:

$$\frac{d\,p}{d\,T} \approx \frac{\Delta\,p}{\Delta\,T} \qquad [1.96]$$

The calculation can be performed between the value on the plateau and the lower or higher value of pressure.

For the first plateau:

$$T = 100\ C = 373.15\ K$$

$$v_V - v_L = 1.6729 - 0.001044 = 1.6718\ m^3\ kg^{-1} \quad [1.97]$$

In "low" values:

$$\Delta p = 101.3 - 84.55 = 16.75\ kPa \quad [1.98]$$

$$\Delta T = 100 - 95 = 5\ C \quad [1.99]$$

In "high" values:

$$\Delta p = 120.82 - 101.3\ = 19.52\ kPa \quad [1.100]$$

$$\Delta T = 105 - 100 = 5\ C \quad [1.101]$$

For the second plateau:

$$T = 225\ C = 498.15\ K$$

$$v_V - v_L = 0.07849 - 0.001199 = 0.07729\ m^3\ kg^{-1} \quad [1.102]$$

In "low" values:

$$\Delta p = 2.548 - 2.318 = 0.23 MPa \quad [1.103]$$

$$\Delta T = 225 - 220 = 5\ C \quad [1.104]$$

In "high" values:

$$\Delta p = 2.795 - 2.548\ = 0.247 MPa \quad [1.105]$$

$$\Delta T = 230 - 225 = 5\ C \quad [1.106]$$

In each of these four cases, the heat of vaporization can be calculated using the expression deduced from Clapeyron's formula:

$$L \approx T\left(v_V - v_L\right)\frac{\Delta p_{Sat}}{\Delta T} \quad [1.107]$$

For the first plateau:

Low values:

$$L \approx T\left(v_V - v_L\right)\frac{\Delta p_{Sat}}{\Delta T} = \frac{373.15*1.6718*16.75.10^3}{5} = 2089\ kJ.kg^{-1} \quad [1.108]$$

High values:

$$L \approx T\left(v_V - v_L\right)\frac{\Delta p_{Sat}}{\Delta T} = \frac{373.15*1.6718*19.52.10^3}{5} = 2435\ kJ.kg^{-1} \quad [1.109]$$

***For the second plateau*:**

Low values:

$$L \approx T\left(v_V - v_L\right)\frac{\Delta p_{Sat}}{\Delta T} = \frac{498.15*0.07729*230.10^3}{5} = 1771\ kJ.kg^{-1} \quad [1.110]$$

High values:

$$L \approx T\left(v_V - v_L\right)\frac{\Delta p_{Sat}}{\Delta T} = \frac{498.15*0.07729*247.10^3}{5} = 1902\ kJ.kg^{-1} \quad [1.111]$$

Let us compare these to the "actual" values.

The values $2089\ kJ.kg^{-1}$ and $2435\ kJ.kg^{-1}$ must be compared to $L = 2257\ \ kJ.kg^{-1}$. The result obtained is within 7 or 8%.

It is important to note that the average $\frac{2089+2435}{2} = 2262\,kJ.kg^{-1}$ gives a significantly better approximation.

$1771\ kJ.kg^{-1}$ and $1902\ kJ.kg^{-1}$ must be compared to $L = 1836,5\ \ kJ.kg^{-1}$. The result obtained is within 3.5%.

It is important to note that the average $\frac{1771+1902}{2} = 1836\,kJ.kg^{-1}$ gives a significantly better approximation.

NOTE.– Given the above notes, it is recommended to calculate the derivative of the pressure using values that frame the studied plateau:

$$\frac{\Delta p_{Sat}}{\Delta T} = \frac{(16.75+19.52)10^3}{10}, \text{ or } \frac{\Delta p_{Sat}}{\Delta T} = \frac{(230+247)10^3}{10} \quad [1.112]$$

EXAMPLE 1.2.– An intriguing bubble

An astute physicist managed to obtain a benzene bubble of diameter $D_1 = 2R_1 = 1cm$ within another water bubble of diameter $D_2 = 2R_2 = 2cm$. The pressure of the ambient air external to the two bubbles is $p_a = 1000\ Pa$. The two bubbles contain air. Within the entire system, there is a constant temperature equal to $T_a = 20C$.

What is the pressure inside the benzene bubble?

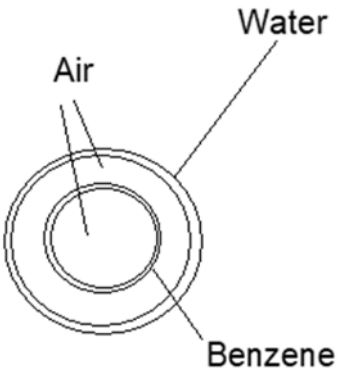

Figure 1.12. *Benzene bubble*

The values of surface tension for water and benzene, which are respectively $\sigma = 7.2.10^{-2}\ N\,m^{-1}$ and $\sigma = 0.44\ N\,m^{-1}$, are given.

SOLUTION TO EXAMPLE 1.2.–

Laplace's formula can be applied to each of the two bubbles. Since there are two interfaces to the bubble, the difference between the internal pressure and the external pressure is:

$$p_i - p_e = \frac{4\sigma}{R} \qquad [1.113]$$

The pressure in the bubble of diameter D_2 is determined using $\sigma = 7.2.10^{-2}\ N\,m^{-1}$:

$$p_{i2} - p_a = \frac{4*7.2.10^{-2}}{10^{-2}} \qquad [1.114]$$

Hence:

$$p_{i2} = 1000 + \frac{4*7.2.10^{-2}}{2.10^{-2}} 1014.4\,Pa \qquad [1.115]$$

The pressure in the bubble of diameter D_1 is determined using $\sigma = 0.44\ N\,m^{-1}$:

$$p_{i1} - p_{i2} = \frac{4*0.44}{10^{-2}} \qquad [1.116]$$

Hence:

$$p_{i2} = 1014.4 + \frac{4*0.44}{10^{-2}} = 1190.4\,Pa \qquad [1.117]$$

EXAMPLE 1.3.– Identification by surface tension

A physicist is in the presence of a liquid. This can be a liquid A or a liquid B. Liquids A and B are indiscernible by their appearance, odor or any other first-hand characteristic.

The only data the physicist has on the liquids A and B are their density and their surface tension.

To discern whether the liquid is an A or a B, the physicist conducts the following experiment.

He pours in a vase a quantity of water, leaving a free surface. He then plunges in this water a transparent tube of unknown diameter. Water rises in the tube. The physicist measures the height of the water in the tube at about 10 mm above the free surface.

He replaces the water in the vase with his unknown liquid. The liquid then rises at about 4 mm above the free surface.

At the beginning and at the end of the experiment, the physicist checks the thermometer in the laboratory. It indicates $20\,C$.

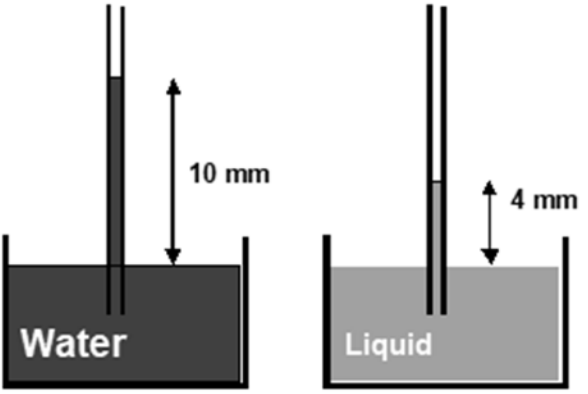

Figure 1.13. *Liquids*

1) Can the physicist state whether he is in the presence of a liquid A or B?

2) In fact, is it possible for him to know the diameter of the tube employed?

The properties of liquids A and B are given below.

Liquid	Surface tension $N.m^{-1}$	Density $kg.m^{-1}$
A	0.025	850
B	0.035	750

SOLUTION TO EXAMPLE 1.3.–

1) Jurin's law can be applied here:

$$h = \frac{4\sigma}{\rho g D} \qquad [1.118]$$

For liquids A and B, the physicist can write using the available data:

– for water:

$$0.1 = \frac{4\sigma_{water}}{10^3\, g\, D} \qquad [1.119]$$

– for the liquid:

$$0.04 = \frac{4\sigma}{\rho\, g\, D} \qquad [1.120]$$

By comparison, knowing that $\sigma_{water} = 7.2.10^{-2}$, they can write:

$$\frac{\sigma\, \rho_{water}}{\sigma_{water}\, \rho} = \frac{0.04}{0.1} \qquad [1.121]$$

or:

$$\frac{\sigma}{\rho} = 0.4 * \frac{7.2.10^{-2}}{10^3} = 2.88.10^{-5}\, N\, m^2\, kg^{-1} \qquad [1.122]$$

To be compared with:

– for liquid A:

$$\frac{\sigma}{\rho} = \frac{0.025}{850} = 2.94.10^{-5}\, N\, m^2\, kg^{-1} \qquad [1.123]$$

– for liquid B:

$$\frac{\sigma}{\rho} = \frac{0.035}{750} = 4.67.10^{-5}\, N\, m^2\, kg^{-1} \qquad [1.124]$$

Within the experimental precision (experiments involving surface tension are always very challenging), the physicist is in the presence of a liquid A.

2) Knowing $\frac{\sigma}{\rho}$, this value can be used in Jurin's law to determine the diameter of the tube; this can be done for water or liquid!

For water:

$$0.1 = \frac{4 * 7.2.10^{-3}}{100\, g\, D} \qquad [1.125]$$

or:

$$D = \frac{4 * 7.2.10^{-2}}{100 * 9.81 * 0.1} = 2.93.10^{-3}\ m = 2.93\ mm \qquad [1.126]$$

EXAMPLE 1.4.– Capillarity and the Eiffel Tower

A somewhat peculiar physicist wants to bring up water from ground level to the top of the Eiffel Tower, without pumping it.

Their setup for this purpose consists of immersing the bottom of a very fine vertical tube of height h, equal to that of the Eiffel Tower, into a water tank.

1) Knowing that starting with 2000 the height of the Eiffel Tower is evaluated at $h = 324\ m$, what should the inner diameter of this tube be?

2) Is the experiment feasible (financial aspects are not considered here)?

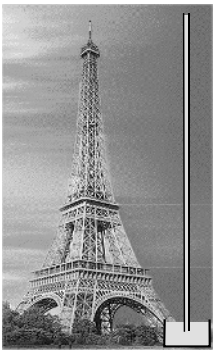

Figure 1.14. *Eiffel Tower*

SOLUTION TO EXAMPLE 1.4.–

1) This problem, which is rather a matter of "entertainment" than of technical study, is an application of Jurin's law:

$$h = \frac{4\sigma}{\rho g D} \qquad [1.127]$$

The standard value $\sigma = 7.2.10^{-2}\ N.m^{-1}$ is considered for the surface tension of water and $\rho = 1000\ kg.m^{-3}$ for the density.

Denoting by D the sought-after diameter, then:

$$D = \frac{4\sigma}{\rho g h} = \frac{4*7.2.10^{-2}}{1000*9.81*324} = 9.06.10^{-8}\ m = 9.06.10^{-2}\ \mu m \qquad [1.128]$$

Or still $90.6.10^{-2}\ nm$!

Manufacturing a capillary of $9.06.10^{-2}\ \mu m$ in diameter appears to be a very challenging task!

EXAMPLE 1.5.– Capillarity rise

A granita wall presents upward leaching up to $h = 40\ cm$ above the ground. What is the porosity of the material?

SOLUTION TO EXAMPLE 1.5.–

The porosity can be defined based on the diameter of the capillary d equivalent to the structure of the material.

Jurin's law can be used to readily calculate, employing the same choices of properties as in the previous problem

$$h = \frac{4\sigma}{\rho g d} \qquad [1.129]$$

or

$$d = \frac{4\sigma}{\rho g h} = \frac{4*7.2.10^{-2}}{1000*9.81*0.4} = 7.34.10^{-5}\ m = 73.4\ \mu m \qquad [1.130]$$

Unlike the previous problem, this is a concrete application!

EXAMPLE 1.6.– The sap rises

It has been assumed for a long time that the sap rises in trees by capillarity in narrow tubes present in the wood structure. Assimilating sap to water, what is the order of magnitude of diameter d of these narrow tubes that would allow the sap to rise from the ground to the highest branch of a tree whose height is 40 m?

SOLUTION TO EXAMPLE 1.6.–

Jurin's law can be used to write, knowing that $\sigma_{water} = 7.2.10^{-2}$ and $\rho = 10^3\ kg\,m^{-3}$

$$h = \frac{4\sigma}{\rho g d} \qquad [1.131]$$

or:

$$40 = \frac{4 * 7.2.10^{-2}}{10^3\ g\,d} \qquad [1.132]$$

Then:

$$d = \frac{4 * 7.2.10^{-2}}{10^3 * 9.81 * 40} = 7.34.10^{-7}\ m = 0.734\ \mu m \qquad [1.133]$$

EXAMPLE 1.7.– Evaporation of a water spray

A water spray is very rapidly introduced in a chamber with air heated at $T_a = 400\,C$.

The drops composing the spray are assumed to all have the same diameter $D_0 = 50\,\mu m$.

The latent heat of vaporization of water is given by

$$L_V = A - BT \qquad [1.134]$$

where: $A = 3334\ kJ\ kg^{-1}$

$$B = 2.9\ kJ\ kg^{-1}K^{-1}$$

At $T = 400\,C$, the thermal conductibility of the air is $\lambda = 0.0509\,W\,m^{-1}\,K^{-1}$ and its specific heat capacity is $c_{PG} = 1004\,J\,Kg^{-1}$.

1) How long does it take for 45% of this spray to evaporate?

2) What is the full vaporization time of this spray?

SOLUTION TO EXAMPLE 1.7.–

1) According to Godsave's law without convection:

$$D^2(t) = D_0^2(t) - K\,t$$

Therefore, the constant K should be calculated:

$$K = 8\frac{\lambda_G}{c_{PG}\rho_L} Ln(1+B) = 8\frac{\lambda_G}{c_{PG}\rho_L} Ln\left(1+\frac{c_{PG}\left(T_V - T_a\right)}{L_V}\right) \qquad [1.135]$$

Here, T_V is the saturation temperature of water, $T_V = 100\,C$ and $T_a = 400\,C$.

Moreover, the latent heat of vaporization of water is:

$$L_V = 3334 - 0.29 * 373 = 2252\,kJ\,kg^{-1}$$

Here, K is given by:

$$K = 8 * \frac{0.0509}{1004 * 1000} Ln\left(1+\frac{1004 * 300}{2252.10^3}\right) \qquad [1.136]$$

$$K = 4.95.10^{-8}\,m^2\,s^{-1}$$

The spray is 45% vaporized when the volume of each drop represents 55% of its initial value. Then, the diameter D of each drop is such that:

$$\left(\frac{D}{D_0}\right)^3 = 0.55 \qquad [1.137]$$

which yields:

$$D = \left(0.55\right)^{1/3} * 50.10^{-6} = 41.10^{-6}\ m \qquad [1.138]$$

This vaporization is obtained at τ_{V1}

$$\tau_{V1} = \frac{D_0^2 - D^2}{K} = \frac{2500.10^{-12} - 1681.10^{-12}}{4.95.10^{-8}} \qquad [1.139]$$

$$\tau_{V1} = 0.0165\,s = 16.5\ ms$$

2) The total time of vaporization τ_{V2} is given by

$$\tau_{V2} = \frac{D_0^2}{K} = \frac{2500.10^{-12}}{4.95.10^{-8}} \qquad [1.140]$$

$$\tau_{V2} = 0.05\,s = 50\,ms$$

EXAMPLE 1.8.– Evaporation of a sodium spray

A sodium spray evaporates in a nitrogen atmosphere at $T_a = 1500\,C$ under a pressure of $76\,cm$ Hg.

This spray has a simple histogram that can be summarized at $t = 0$ through a distribution between four sizes of drops.

For 100 drops of spray:

Diameter of the drop in micron	**Number within size for 100 drops**
10	**15**
50	**35**
100	**35**
200	**15**

1) What is the temperature at the surface of sodium drops under evaporation?

2) What is the vaporization constant K of the sodium drops?

3) What is the numerical mean diameter of this distribution, d_{10} at the moment $t = 0$?

4) Consider this spray after $\tau_V = 240\ ms$.

What is the new distribution for 100 drops? It is recommended to calculate the evolution of the drop sizes starting with the largest size class.

5) For this new distribution, what are at the moment $t = \tau_V$, the numerical mean diameter (d_{10}), volume mean diameter (d_{30}) and Sauter mean diameter or SMD (d_{32})?

Given:

Density of liquid sodium: $\rho_L = 927\ kg\ m^{-3}$

Enthalpy of vaporization of sodium: $L_V = 96.96\ kJ\ mol^{-1}$

Heat capacity of air: $c_{PG} = 1004\ J\ kg^{-1}$

Thermal conductibility of air: $\lambda_G = 0.024\ W\ m^{-1}\ K^{-1}$

Given: $Na = 23$

The melting temperature of sodium is $T_f = 371\ K$.

SOLUTION TO EXAMPLE 1.8.–

1) The surface of drops is at the melting temperature:

$$T_f = 371\ K = 98\ C$$

2) The evolution of the size of each droplet is given by the D^2 -law:

$$D^2(t) = D_0^2(t) - K\,t \qquad [1.141]$$

The sodium vaporization constant can be calculated as:

$$K = 8\frac{\lambda_G}{c_{PG}\rho_L} Ln(1+B) = 8\frac{\lambda_G}{c_{PG}\rho_L} Ln\left(1+\frac{c_{PG}\left(T_V - T_a\right)}{L_V}\right) \qquad [1.142]$$

The heat of vaporization can be deduced from the enthalpy of vaporization per mole, whose mass is $M = 23\,g = 23.10^{-3}\,kg$

$$L_V = \frac{96.96.10^3}{23.10^{-3}} = 4.21.10^6\,J\,kg^{-1} \qquad [1.143]$$

K is:

$$K = 8\frac{0,024}{1004*927}Ln\left(1+\frac{1004*\left(T_V - T_a\right)}{4.21.10^6}\right) = 5.94.10^{-8} \qquad [1.144]$$

3) According to the definition of mean diameters:

$$d_{pq} = \int_0^\infty \left[\frac{x^p\, f_n(x)}{x^q\, f_n(x)}\right]^{\frac{1}{p\_q}} d\,x \qquad [1.145]$$

then:

$$d_{10} = \int_0^\infty x\, f_n(x)\delta x \qquad [1.146]$$

The histogram over drops can be used to readily determine a table of the distribution function:

Drop diameter size in micron	**Number in the size** $f_n(x)$
10	**0.15**
50	**0.35**
100	**0.35**
200	**0.15**

Hence, the numerical mean diameter:

$$d_{10} = (0.15*10) + (0.35*50) + (0.35*100) + (0.15*200) = 84\,\mu m \qquad [1.147]$$

4) After $t = \tau_V = 240.10^{-3}\,s$, the size per class of drops can be calculated using $K = 5.94.10^{-8}$.

Initial size of $200\,\mu m$:

$$D^2 = \left(200.10^{-6}\right)^2 - 5.94.10^{-8} * 0.24 = 2.57.10^{-8} \qquad [1.148]$$

$$D = 1.6.10^{-4}\ m = 160\,\mu m$$

Initial size of $100\,\mu m$:

$$D^2 = \left(100.10^{-6}\right)^2 - 5.94.10^{-8} * 0.24 = 4.26.10^{-9}$$

$$D = 6.53.10^{-5}\ m = 65.3\,\mu m$$

Initial size of $50\,\mu m$:

$$D^2 = \left(50.10^{-6}\right)^2 - 5.94.10^{-8} * 0.24 = -1.17.10^{-8}$$

This negative result makes no physical sense; in fact, the class $D = 50\,\mu m$ is fully vaporized. This can be verified by calculating the vaporization time:

$$t_{V50} = \frac{D_0^2}{K} = \frac{\left(50.10^{-6}\right)^2}{5.94.10^{-8}} = 4.21.10^{-2}\ s = 42.1 ms \qquad [1.149]$$

Obviously, class $D = 50\,\mu m$ will also be fully vaporized.

The histogram of the final spray is then:

Size micron	Number
65.3	**35**
160	**15**

This makes it possible to calculate the numerical distribution function:

Size micron	$f_n(x)$
65.3	**0.70**
160	**0.30**

Mean diameters can then be readily calculated:

– numerical mean diameter:

$$d_{10} = (0.7 * 65.3) + (0.3 * 160) = 92.1\,\mu m \qquad [1.150]$$

– volume mean diameter:

$$d_{10} = \left\{ \left[0.7 * (65.3)^3 \right] + \left[0.3 * (160)^3 \right] \right\}^{\frac{1}{3}} = 112.5\,\mu m \qquad [1.151]$$

– Sauter mean diameter:

$$d_{32} = \frac{\left[0.7 * (65.3)^3 \right] + \left[0.3 * (160)^3 \right]}{\left[0.7 * (65.3)^2 \right] + \left[0.3 * (160)^2 \right]} = 68.1\,\mu m \qquad [1.152]$$

EXAMPLE 1.9.– Bubble dynamics

This problem requires a purely analytical resolution. There are no numerical values to be considered.

The evolution of a bubble in a liquid is considered. This bubble is *exclusively filled with vapor* of this liquid at the saturation vapor pressure.

The following are considered negligible:

– viscosity effects;

– surface tension effects.

The bubble is initially at equilibrium with a radius R_0. The ambient pressure is then $p_{\infty 0}$.

The ambient pressure follows the law:

$$p_\infty(t) = p_V - p_{\infty 0} \exp(2\alpha t) \qquad [1.153]$$

p_V, pressure of vapor at the temperature of the experiment is the pressure in the bubble.

1) Considering the previous hypotheses, what is the differential equation describing the temporal evolution $R(t)$ of the radius of the bubble?

2) It can be noted that the radius of the bubble $R(t)$ will have the form:

$$R(t) = A\exp(2\alpha t) \qquad [1.154]$$

where A is a constant. Determine A.

What can be said about the initial radius R_0?

SOLUTION TO EXAMPLE 1.9.–

1) The Rayleigh–Plesset equation describes the evolution of the radius of a bubble submitted to an ambience $p_\infty(t)$; without simplifying the hypotheses, it is written as:

$$R\frac{d^2R}{dt^2} + \frac{3}{2}\left(\frac{dR}{dt}\right)^2 + \frac{4\nu_L}{R}\frac{dR}{dt} + \frac{2\sigma}{\rho_L R} + \frac{\Delta p(t)}{\rho_L} = 0 \qquad [1.155]$$

Neglecting the effects of viscosity and surface tension, it is written as:

$$R\frac{d^2R}{dt^2} + \frac{3}{2}\left(\frac{dR}{dt}\right)^2 + \frac{p_\infty(t) - p_V}{\rho_L} = 0 \qquad [1.156]$$

with the boundary conditions:

$$t = 0 \quad ; \quad R = R_0$$

2) Intuitively, the solution to be found has the form:

$$R = A\exp\beta t$$

Noting that:

$$p_\infty(t) - p_V = -p_{\infty 0}\exp 2\alpha t \qquad [1.157]$$

and:

$$\frac{d\,R}{d\,t} = A\beta \exp \beta t \qquad [1.158]$$

$$\frac{d^2 R}{d\,t^2} = A\beta^2 \exp \beta t \qquad [1.159]$$

the simplified Rayleigh–Plesset equation is written as:

$$A e^{\beta t}\ A\beta^2 e^{\beta t} + \frac{3}{2}\left(A\beta e^{\beta t}\right)^2 \ = \frac{p_{\infty 0}\, e^{2\alpha t}}{\rho_L} \qquad [1.160]$$

Let:

$$A^2\beta^2 e^{2\beta t} + \frac{3}{2} A^2\beta^2 e^{2\beta t 2} \ = \frac{p_{\infty 0}\, e^{2\alpha t}}{\rho_L} \qquad [1.161]$$

and by identifying:

$$\alpha = \beta$$

$$\frac{5}{2} A^2\beta^2 = \frac{5}{2} A^2\alpha^2 = \frac{p_{\infty 0}}{\rho_L} \qquad [1.162]$$

$$\frac{5}{2} A^2\beta^2 = \frac{5}{2} A^2\alpha^2 = \sqrt{\frac{2p_{\infty 0}}{5\rho_L\alpha^2}} \qquad [1.163]$$

Hence:

$$R(t) = \sqrt{\frac{2p_{\infty 0}}{5\rho_L\alpha^2}} \exp 2\alpha t \qquad [1.164]$$

The value of the initial radius is:

$$R_0 = \sqrt{\frac{2p_{\infty 0}}{5\rho_L\alpha^2}} \qquad [1.165]$$

Therefore, R_0 and α cannot be independent.